

*Appendix A***OVERVIEW OF THE FOCUSED ISOPRENE EXPERIMENT AT THE CALIFORNIA INSTITUTE OF TECHNOLOGY (FIXCIT): MECHANISTIC CHAMBER STUDIES ON THE OXIDATION OF BIOGENIC COMPOUNDS**

Nguyen, T. B., J. D. Crouse, R. H. Schwantes, A. P. Teng, K. H. Bates, X. Zhang, J. M. St. Clair, W. H. Brune, G. S. Tyndall, F. N. Keutsch, J. H. Seinfeld, and P. O. Wennberg (2014). “Overview of the Focused Isoprene eXperiment at the California Institute of Technology (FIXCIT): Mechanistic chamber studies on the oxidation of biogenic compounds”. In: *Atmos. Chem. Phys.* 14.24, pp. 13531–13549. DOI: 10.5194/acp-14-13531-2014.

**Abstract**

The Focused isoprene eXperiment at the California Institute of Technology (FIXCIT) was a collaborative atmospheric chamber campaign that occurred during January 2014. FIXCIT is the laboratory component of a synergistic field and laboratory effort aimed toward (1) better understanding the chemical details behind ambient observations relevant to the southeastern United States, (2) advancing the knowledge of atmospheric oxidation mechanisms of important biogenic hydrocarbons, and (3) characterizing the behavior of field instrumentation using authentic standards. Approximately 20 principal scientists from 14 academic and government institutions performed parallel measurements at a forested site in Alabama and at the atmospheric chambers at Caltech. During the 4 week campaign period, a series of chamber experiments was conducted to investigate the dark- and photo-induced oxidation of isoprene,  $\alpha$ -pinene, methacrolein, pinonaldehyde, acylperoxy nitrates, isoprene hydroxy nitrates (ISOPN), isoprene hydroxy hydroperoxides (ISOPOOH), and isoprene epoxydiols (IEPOX) in a highly controlled and atmospherically relevant manner. Pinonaldehyde and isomer-specific standards of ISOPN, ISOPOOH, and IEPOX were synthesized and contributed by campaign participants, which enabled explicit exploration into the oxidation mechanisms and instrument responses for these important atmospheric compounds. The present overview describes the goals, experimental design, instrumental techniques, and preliminary observations from the campaign. This work provides context for forthcoming publications affiliated with the FIXCIT campaign. Insights from FIXCIT are anticipated to aid

significantly in interpretation of field data and the revision of mechanisms currently implemented in regional and global atmospheric models.

## A.1 Introduction

### A.1.1 Background

Biogenically produced isoprenoids (hydrocarbons comprised of  $C_5H_8$  units) have global emission rates into the atmosphere surpassing those of anthropogenic hydrocarbons and methane (Guenther *et al.*, 2012; Guenther *et al.*, 1995). The biogenic carbon emission flux is dominated by isoprene ( $C_5H_8$ ) and monoterpenes ( $C_{10}H_{16}$ ), which account for approximately 50% and 30% of the OH reactivity over land, respectively (Fuentes *et al.*, 2000). Furthermore, it has been suggested that the atmospheric oxidation of isoprene, in particular, can buffer the oxidative capacity of forested regions by maintaining levels of the hydroxyl radical (OH) under lower nitric oxide (NO) conditions (Lelieveld *et al.*, 2008). Due to their large abundances, isoprene and monoterpenes also dominate the global budget of secondary organic aerosol (SOA) (Henze *et al.*, 2008). Thus, the accurate representation of detailed chemistry for isoprene and monoterpene is necessary for meaningful simulations of atmospheric  $HO_x$  (OH +  $HO_2$ ),  $NO_x$  (NO +  $NO_2$ ), surface ozone ( $O_3$ ), trace gas lifetimes, and SOA.

Unsaturated hydrocarbons like isoprene and monoterpenes are primarily oxidized by OH,  $O_3$ , and the nitrate ( $NO_3$ ) radical in the atmosphere. OH oxidation is the dominant fate for isoprene, but  $O_3$  and  $NO_3$  oxidation can dominate reactivity for monoterpenes and sesquiterpenes. Our understanding of the OH-initiated isoprene oxidation mechanism has significantly improved during the last decade, following the first suggestion of the capacity of isoprene to produce SOA (Claeys *et al.*, 2004). The mechanistic developments have been propelled by technological advancements in instrumentation (Crouse *et al.*, 2006; Hansel *et al.*, 1995; Jordan *et al.*, 2009; Junninen *et al.*, 2010), enabling the detection of more complex oxidation products derived from isoprene and other biogenic hydrocarbons. However, the scientific understanding of these biogenic oxidation mechanisms is far from complete. It is outside the scope of this overview to describe comprehensively the isoprene and monoterpene oxidation mechanisms. Rather, we provide a brief background of the oxidation of biogenic hydrocarbons, which includes "state-of-the-science" knowledge, to motivate the study. The mechanisms described here are illustrated in Figure A.1.

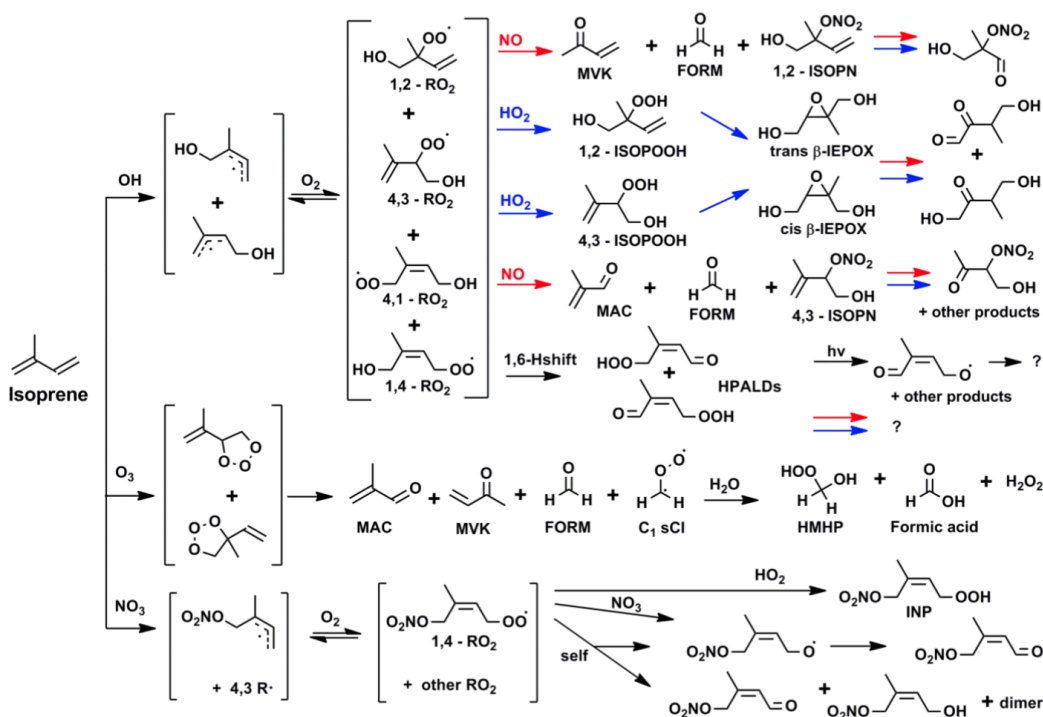


Figure A.1: Representative mechanism from the OH-, O<sub>3</sub>- and NO<sub>3</sub>-initiated oxidation of isoprene. The most abundant isomers of a particular pathway are shown. Red and blue arrows in the OH-oxidation scheme denote the NO-dominated and HO<sub>2</sub>-dominated RO<sub>2</sub> reactions, respectively. For the ozonolysis reaction, only the C<sub>1</sub> SCI and its reaction with water are shown as further-generation chemistry. For the NO<sub>3</sub>-oxidation pathway, only one isomer each of R and RO<sub>2</sub> radicals is shown for brevity. Abbreviations are defined in the text.

#### A.1.1.1 OH Oxidation

OH predominantly adds to either of the double bonds of isoprene, followed by the reversible addition of O<sub>2</sub> (Peeters *et al.*, 2009) to produce several isomers of alkylperoxyl radicals (RO<sub>2</sub>). In the atmosphere, these RO<sub>2</sub> react mainly with HO<sub>2</sub> and NO to form stable products, although self-reaction can be non-negligible under certain conditions. The stable products are often termed oxidized volatile organic compounds (OVOCs). In urban-influenced areas, the "high-NO" pathway is more important and in more pristine environments, the "low-NO" or HO<sub>2</sub>-dominated pathway is more important. The high-NO pathway generates isoprene hydroxy nitrates (ISOPN) that act as reservoirs for NO<sub>x</sub>, as well as other products such as methyl vinyl ketone (MVK), methacrolein (MAC), and hydroxyacetone (HAC) (Paulot *et al.*, 2009a). For conditions with sufficiently high NO<sub>2</sub>-to-NO ratios, as is mainly the case in the atmospheric boundary layer outside of cities, methacryloyl

peroxynitrate (MPAN) is formed from the photooxidation of MAC. Further oxidation of MPAN can generate SOA (Chan *et al.*, 2010a; Surratt *et al.*, 2010). The low-NO pathway generates isoprene hydroxy hydroperoxides (ISOPOOH) in almost quantitative yields, and further OH oxidation of ISOPOOH produces the epoxydiols in an OH-conserving mechanism (Paulot *et al.*, 2009b). In unpolluted atmospheres, when the RO<sub>2</sub> lifetimes are sufficiently long (~100 s in a forest), isomerization of the RO<sub>2</sub> followed by reaction with O<sub>2</sub> becomes an important fate, producing the isoprene hydroperoxy aldehydes (HPALDs) and other products (Crouse *et al.*, 2011; Peeters *et al.*, 2009). These RO<sub>2</sub> isomerization reactions are a type of rapid oxygen incorporation chemistry (Crouse *et al.*, 2013; Ehn *et al.*, 2014; Vereecken *et al.*, 2007) that is thought to be responsible for the prompt generation of low-volatility SOA components. Further generations of OH oxidation in isoprene are currently being explored owing to recent success with chemical syntheses of important OVOCs (Bates *et al.*, 2014; Jacobs *et al.*, 2013; Lee *et al.*, 2014; Wolfe *et al.*, 2012). It has been found that the OH oxidation of IEPOX and ISOPN, surprisingly under both low-NO and high-NO conditions, results primarily in fragmentation of the C<sub>5</sub> skeleton.

Despite extensive work on the isoprene + OH mechanism, large uncertainties persist, some of which directly translate into uncertainties in atmospheric model predictions. These uncertainties stem from, for example, the large range in reported yields for isoprene nitrates (4–15%) (Paulot *et al.*, 2009a), disagreements up to 90% in reported MAC and MVK yields from the low-NO pathway (Liu *et al.* (2013), and references therein), various proposed sources of SOA from the high-NO pathway (Chan *et al.*, 2010a; Kjaergaard *et al.*, 2012; Lin *et al.*, 2013b), missing contributions to SOA mass from the low-NO pathway (Surratt *et al.*, 2010), uncharacterized fates of oxidized species like HPALDs (which may have isomer dependence), incomplete understanding of oxygen incorporation (Crouse *et al.*, 2013; Peeters *et al.*, 2009), and under-characterized impact of RO<sub>2</sub> lifetimes on chamber results (Wolfe *et al.*, 2012). The OH oxidation of  $\alpha$ -pinene (Eddingsaas *et al.*, 2010) and other monoterpenes is less well characterized than that of isoprene, but, in general, proceeds through analogous steps.

#### A.1.1.2 Ozone Oxidation

Ozonolysis is a significant sink for unsaturated hydrocarbons and a large nighttime source of OH, particularly in urban-influenced areas. Reaction with ozone is

more important for monoterpenes than isoprene, due to the faster rate coefficients (Atkinson and Lloyd, 1984) and the nighttime emission profile for the monoterpenes. Furthermore, monoterpene ozonolysis is highly efficient at converting VOC mass to SOA (Griffin *et al.*, 1999; Hoffmann *et al.*, 1997). There is a general consensus that ozonolysis occurs *via* the Criegee mechanism (Criegee, 1975), wherein ozone adds to a hydrocarbon double bond to form a five-member primary ozonide that quickly decomposes to a stable carbonyl product and an energy-rich Criegee intermediate (CI). In  $\alpha$ -pinene oxidation, ozonolysis, NO<sub>3</sub>-initiated, and OH-initiated reactions all produce pinonaldehyde (C<sub>10</sub>H<sub>16</sub>O<sub>2</sub>) as a major product (Atkinson and Arey, 2003b; Wängberg *et al.*, 1997), whereas major first-generation products from isoprene ozonolysis include MAC, MVK, and formaldehyde. The "hot" Criegee can promptly lose OH (Kroll *et al.*, 2001) while ejecting an alkyl radical, or become stabilized by collision with atmospheric gases to form a stabilized Criegee intermediate (sCI) with long enough lifetimes to react bimolecularly. The subsequent reactions of sCIs produce both carbonyl products and non-carbonyl products such as hydroperoxides. The *syn* and *anti* conformers of CIs and SCI can have substantially different reactivities (Anglada *et al.*, 2011; Kuwata *et al.*, 2010), with *syn* conformers more likely to decompose unimolecularly, possibly through a vinyl hydroperoxide intermediate (Donahue *et al.*, 2011).

It has been suggested that reaction with water molecules is a major (if not dominant) bimolecular fate of SCI in the atmosphere due to the overwhelming abundance of atmospheric water (Fenske *et al.*, 2000). This suggestion is supported by observations of high mixing ratios (up to 5 ppbv) of hydroxymethyl hydroperoxide (HMHP), a characteristic product of reactions of the smallest SCI (CH<sub>2</sub>OO) with water (Neeb *et al.*, 1997), over forested regions and in biomass burning plumes (Gab *et al.*, 1985; Lee and Hsu, 2000; Lee *et al.*, 1993a; Valverde-Canossa *et al.*, 2006). Although HMHP and other hydroperoxides produced from ozonolysis are important atmospheric compounds, their yield estimates are highly uncertain (Becker *et al.*, 1990; Hasson *et al.*, 2001a; Huang *et al.*, 2013; Neeb *et al.*, 1997; Sauer *et al.*, 1999). This may be attributable to the fact that hydroperoxide yields have mainly been determined by offline methods or under conditions with highly elevated hydrocarbon loadings. Furthermore, few empirical data exist on the humidity dependence of product branching in this reaction. Lastly, the rate coefficients for the SCI + H<sub>2</sub>O reaction, and other SCI reactions, are still uncertain by several orders of magnitude (Johnson and Marston, 2008; Welz *et al.*, 2012), precluding the assessment of their atmospheric importance.

### A.1.1.3 Nitrate Oxidation

NO<sub>3</sub> oxidation also produces RO<sub>2</sub> radicals by addition to alkenes in the presence of O<sub>2</sub>. Owing to its high reaction rate coefficient coupled to atmospheric abundance,  $\alpha$ -pinene is expected to be an important sink for NO<sub>3</sub> in many areas. The NO<sub>3</sub>-derived RO<sub>2</sub> radicals react with (a) NO<sub>3</sub> to form alkoxy radicals (RO) that lead primarily to the production of nitrooxy carbonyls (b); with other RO<sub>2</sub> radicals to form RO radicals, nitrooxy carbonyls, hydroxy nitrates, and nitrooxy peroxy dimers; and (c) with HO<sub>2</sub> to form nitrooxy hydroperoxides. Further generation NO<sub>3</sub>-oxidation produces dinitrates, amongst other products. As the NO<sub>3</sub> addition initiates the reaction, the thermodynamically preferred organic hydroxy nitrates produced through nighttime oxidation may be structurally different than those produced in the daytime through OH oxidation. During nighttime oxidation, tropospheric HO<sub>2</sub> mixing ratios often surpass those of NO<sub>3</sub> (Mao *et al.*, 2012), implying HO<sub>2</sub> reaction to be a common fate for NO<sub>3</sub>-derived RO<sub>2</sub>. However, previous studies of this reaction have maintained conditions where minimal HO<sub>2</sub> + RO<sub>2</sub> chemistry occurs and the dominant fate of RO<sub>2</sub> is reaction with NO<sub>3</sub> and RO<sub>2</sub> (Kwan *et al.*, 2012; Ng *et al.*, 2008; Perring *et al.*, 2009; Rollins *et al.*, 2009). This may be one of the reasons why nitrooxy hydroperoxides (the RO<sub>2</sub> + HO<sub>2</sub> product) are observed with much higher relative abundances in ambient air (Beaver *et al.*, 2012) than in chamber studies.

### A.1.2 Scientific Goals

The 2014 Focused isoprene eXperiment at the California Institute of Technology (FIXCIT) is a collaborative atmospheric chamber campaign focused on advancing the understanding of biogenic hydrocarbon oxidation in the atmosphere. The campaign was motivated by the communal need for a tight coupling of field and laboratory efforts toward understanding the mechanistic details responsible for ambient observations, exploring explicit chemistry as driven by the fate of RO<sub>2</sub> radicals through well-controlled experiments, and fully characterizing instrumental response to important trace gases using authentic standards to guide data interpretation. To accomplish these goals, a suite of instruments typically deployed for field missions was used to perform parallel measurements at a forested site in Alabama and then in the atmospheric chambers at Caltech. This overview provides an account of the goals and conditions for the experiments performed during the campaign. A key component of FIXCIT is the re-design of "typical chamber experiments" to recreate the ambient atmosphere with higher fidelity so that results from laboratory studies can be implemented in models and used to interpret ambient observations with

higher confidence.

### A.1.2.1 Understanding Ambient Observations

FIXCIT was designed as a sister investigation to the 2013 Southern Oxidant and Aerosol Study (SOAS). During SOAS (June-July 2013), a select sub-suite of instruments recorded ambient observations above the forest canopy on top of a metal walk-up tower 20 m in height. The sampling site, located in Brent, Alabama at the Centreville (CTR) SEARCH location managed by the Electric Power Research Institute (CTR: 32.90289 ° N, 87.24968° W), was surrounded by a temperate mixed forest (part of the Talladega National Forest) that was occasionally impacted by anthropogenic emission. CTR was characterized by high atmospheric water content (2.4–3 vol.% typically), elevated temperatures (28–30 °C during the day), high SOA loadings (particulate organics  $\sim 4\text{--}10 \mu\text{g m}^{-3}$ ; sulfate  $\sim 2 \mu\text{g m}^{-3}$ ), high isoprene mixing ratios (4–10 ppbv), high ozone (40–60 ppbv), low-to-moderate nitrogen oxides ([NO]  $\sim 0.3\text{--}1.5$  ppbv, [NO<sub>2</sub>]  $\sim 1\text{--}5$  ppbv), occasional plumes of SO<sub>2</sub> from nearby power plants, and occasional biomass burning events during the SOAS campaign.

The first goal of the chamber campaign was to further investigate the more interesting observations at SOAS. Due to the ability of laboratory experiments to study the chemistry of a single reactive hydrocarbon in a controlled setting, it was possible to test hypotheses during FIXCIT in a systematic manner. Below we list some relevant questions from the SOAS campaign that were explored during FIXCIT.

1. Which reactions or environmental conditions control the formation and destruction of OVOCs in the southeastern US?
2. Are RO<sub>2</sub> isomerization and other rapid oxygen incorporation mechanisms of key hydrocarbons important during SOAS?
3. How do anthropogenic influences, *e.g.* NO<sub>x</sub>, O<sub>3</sub>, and (NH<sub>4</sub>)<sub>2</sub>SO<sub>4</sub>, impact atmospheric chemistry over the forest?
4. How much does the NO<sub>3</sub>-initiated reaction control nighttime chemistry during SOAS?
5. How do environmental conditions in the southeastern US affect ozonolysis end products, which are known to be water sensitive?

6. Which reactions or environmental conditions most significantly impact SOA mass and composition?

#### **A.1.2.2 Updating the isoprene and Monoterpene Mechanisms**

Several experiments were designed to "fill in the gaps" of the isoprene oxidation mechanisms by leveraging the comprehensive collection of sophisticated instrumentation at FIXCIT. We targeted the following acknowledged open questions.

7. What are the products of the photochemical reactions stemming from OVOCs like ISOPOOH, IEPOX, ISOPN, and pinonaldehyde?

8. What is the impact of photolysis vs. photooxidation for photolabile compounds?

9. What is the true yield of isoprene nitrates from the high NO photooxidation pathway?

10. What is the product distribution and true yield of nitrooxy hydroperoxides from the NO<sub>3</sub> oxidation reaction of isoprene and monoterpenes under typical atmospheric conditions?

11. How do products and yields change as RO<sub>2</sub> lifetimes in chamber studies approach values estimated to be prevalent in the troposphere?

#### **A.1.2.3 Instrument Characterization**

A final goal of FIXCIT was to evaluate, compare, and identify biases in field instrumentation by isolating one variable at a time. We focused on the following objectives.

12. Identify the causal factor(s) producing the "OH interference" (Mao *et al.*, 2012) that has been observed in various biogenically impacted regions by some gas-expansion laser-induced fluorescence (LIF) techniques.

13. Characterize the performance of newly commercially available CIMS instrumentation with respect to the detection of OVOCs by using authentic standards.

14. Compare similar measurements (*e.g.* OH reactivity, hydrocarbons, OVOCs) made with different techniques.



## A.2 Scope of the Campaign

### A.2.1 Facilities

Experiments were performed in the Caltech Atmospheric Chamber Facility within a 1 month period in January 2014. The facility contains several in-house gas- and aerosol-phase instruments and an  $8 \times 5$  m insulated enclosure, housing two side-by-side Teflon atmospheric chambers that are suspended from the ceiling. The chambers were manufactured from fluorinated ethylene propylene (FEP) Teflon. The chamber volume was measured regularly by quantitative transfer of highly volatile organics such as isoprene by an externally calibrated GC-FID. Quantitative transfer was checked *via* injections of a measured quantity of isoprene (checked by gravimetric, volumetric, and FT-IR methods) into a pillow bag with known volume by timing a calibrated mass flow of air into the pillow bag. For most experiments, the chamber volume was between 23 and 24 m<sup>3</sup>. The spatial configuration of instruments in the chamber facility during FIXCIT is shown in Figure A.2. The instruments, contributors, and identifying abbreviations used in this work are described in Table A.1. A total of 320 UV black lamps (broadband  $\lambda_{max} \sim 350$  nm) are mounted on the walls of the enclosure. The lamps are located behind Teflon films so that the heat produced from the operation of the lamps can be removed by recirculating cool air. The interior of the enclosure is covered with reflective aluminum sheets. Light intensities can be tuned to 100, 50, 10, and 1%.  $J_{NO_2}$  was measured to be  $7 \times 10^{-3}$  s<sup>-1</sup> at 100% light intensity. Light fluxes at several locations within the chamber (*e.g.* center, corner, right, left, high, low) did not vary more than 15%. Temperature controls in the chamber enclosure are tunable from 10 to 50 °C (typically set at 25 °C) and did not fluctuate more than 1 °C, except during periods when the temperature was explicitly changed or during a 30 min period immediately following a change in the light intensities (up to 2 °C increase was observed from switching on 100% lights.)

The chamber experiments were operated in batch mode throughout the campaign. Temperature and RH were monitored continuously inside the chamber by a Vaisala HMM211 probe calibrated with saturated salt solutions in the RH range of 11–95%. In the range RH < 11%, water vapor measurements were provided by the TripCIMS. The chambers were flushed at least 24 h before each use with ultra-purified air (purified in-house *via* a series of molecular sieves, activated carbon, Purafil<sup>TM</sup> media, and particulate filters), at elevated temperature when needed ( $\sim 40$  °C), so that the backgrounds on gas- and particle-phase instrumentation are at baseline levels. As a reference, NO levels before each run were typically less than 100

instrument	instr. ID	PI(s)	institutions	measurements	ref.
Ground-based hydrogen oxide sensor	GTHOS	W. H. Brune	PA State Univ. (PSU)	OH, HO <sub>2</sub> , RO <sub>2</sub>	a
LIF OH reactivity monitor	LIF-OHR	W. H. Brune	PSU	OH reactivity by decay of OH	b
Thermal dissociation LIF NO <sub>2</sub> monitor	TDLIF	R. C. Cohen	Univ. of CA, Berkeley (UCB)	NO <sub>2</sub> , sum of org. nitrates (ΣANs), sum of peroxy nitrates (ΣPNs), particulate org. nitrates (pANs)	c
Switchable iodide and acetate ion HRTof-CIMS	IACIMS	D. K. Farmer	CO State Univ. (CSU)	Oxidized VOCs (organic nitrates, acids, <i>etc.</i> )	d
NO <sub>3</sub> HRTof-CIMS	NO <sub>3</sub> CIMS	M. R. Canagaratna, D. R. Worsnop, J. L. Jimenez	Aerodyne Research, Inc. (ARI) and Univ. of CO, Boulder (CUB)	Low-volatility organic compounds	e
LIP glyoxal monitor	GlyLIP	F. N. Keutsch	Univ. of WI, Madison (UWM)	glyoxal	f
LIF formaldehyde monitor	FormLIF	F. N. Keutsch	UWM	Formaldehyde	g
Comparative rate method OH reactivity monitor	CRM-OHR	S. Kim, A. B. Guenther	Univ. of CA, Irvine (UCI) and Pacific NW National Lab (PNNL)	OH reactivity by decay of hydrocarbons	h
Switchable reagent ion (H <sub>3</sub> O <sup>+</sup> /NO <sup>+</sup> /O <sub>2</sub> <sup>+</sup> ) HRTof-MS	SRI-ToFMS	A. B. Guenther, J. E. Mak, A. H. Goldstein	PNNL, SUNY Stonybrook (SUNY), and UCB	Hydrocarbons, carbonyls, alcohols, <i>etc.</i>	i
Chemical luminescence NO monitor	NO-CL	G. S. Tyndall, D. D. Montzka, A. J. Weinheimer	National Center for Atmospheric Research (NCAR)	NO (> 25 pptv)	j
CF <sub>3</sub> O <sup>-</sup> triple quadrupole CIMS	TripCIMS	P. O. Wennberg	CA Institute of Technology (Caltech)	ISOPOOH, IEPOX, glycolaldehyde, acetic acid, methyl hydroperoxide	k
CF <sub>3</sub> O <sup>-</sup> CToF-CIMS	ToFCIMS	P. O. Wennberg	Caltech	Oxygenated VOCs (hydroperoxides, organic nitrates, multi-functional compounds)	l
Gas chromatograph with ToFCIMS	GC-ToFCIMS	P. O. Wennberg	Caltech	Isomers for oxygenated VOCs	m
HRTof-aerosol mass spectrometer	ToF-AMS	J. H. Seinfeld	Caltech	Aerosol composition and size distribution	n
Gas chromatograph with flame-ionization detector	GCFID	J. H. Seinfeld	Caltech	isoprene, methacrolein, MVK, cyclohexane	N/A
Thermocouple and membrane probe	T /RH probe	J. H. Seinfeld	Caltech	Temperature and relative humidity	N/A
UV-absorption ozone monitor	O <sub>3</sub> monitor	J. H. Seinfeld	Caltech	O <sub>3</sub> (> 1000 pptv)	N/A
Chemical luminescence NO <sub>x</sub> detector	NO <sub>x</sub> monitor	J. H. Seinfeld	Caltech	NO (> 500 pptv), and NO <sub>2</sub> (catalytic conversion to NO)	N/A

Table A.1: List of participating instruments, principle investigators (PIs), and institutions. Key acronyms: laser-induced fluorescence (LIF), laser-induced phosphorescence (LIP), high-resolution time-of-flight (HRTof), compact time-of-flight (CTof), MS (mass spectrometer), and CIMS (chemical ionization mass spectrometer). References listed are: <sup>a</sup>Brune *et al.* (1995), <sup>b</sup>Mao *et al.* (2009), <sup>c</sup>Day *et al.* (2002), <sup>d</sup>Lee *et al.* (1993b), <sup>e</sup>Junninen *et al.* (2010), <sup>f</sup>Huisman *et al.* (2008), <sup>g</sup>DiGangi *et al.* (2011) and Hottle *et al.* (2009), <sup>h</sup>Sinha *et al.* (2008), <sup>i</sup>Jordan *et al.* (2009), <sup>j</sup>Ridley and Grahek (1990), <sup>k</sup>St. Clair *et al.* (2010), <sup>l</sup>Crouse *et al.* (2006), <sup>m</sup>Bates *et al.* (2014), and <sup>n</sup>Canagaratna *et al.* (2007) and DeCarlo *et al.* (2006).

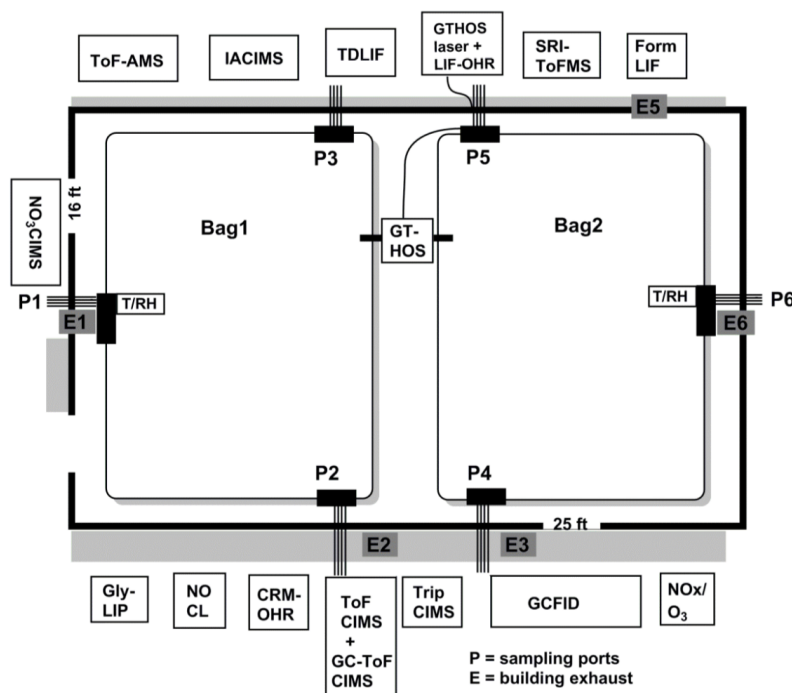


Figure A.2: Arrangement of instruments at the Caltech Atmospheric Chamber Facility during the campaign. Instrument IDs are in Table A.1.

pptv (from NO-CL measurements) and particle concentrations were less than  $0.01 \mu\text{g m}^{-3}$ . Flushing rates, as balanced by exhaust rates, were typically  $250 \text{ SD L min}^{-1}$  (SLM) or  $\sim 0.6$  chamber volumes per hour. Chambers were mixed on the timescale of minutes by injecting high-pressure pulses of air during the beginning of experiments.

Chamber 1 was reserved for low-NO experiments, so that the walls did not contact elevated levels of nitric acid and organic nitrates during the lifetime of the chamber, while Chamber 2 was reserved for moderate- to high-NO experiments. Experiments were carried out daily in alternating chambers to allow for the full flushing period of the previously used chamber. Each chamber was characterized separately prior to the campaign for vapor and particle wall loss rates. Typically, wall loss rates for gas-phase species are slightly higher in the high-NO chamber than the low-NO chamber due to the greater acidity of the walls. Particle wall loss rates were not significantly different between chambers. Measurements of the particle wall loss rates were performed by injecting ammonium sulfate (AS) seed aerosols into the chamber and monitoring the decay over the course of 10–24 h. Particles were injected *via* atomization of dilute salt solutions (*e.g.* AS 0.06 M) through a  $^{210}\text{Po}$  neutralizer and water trap. Measurements of vapor wall loss rates were performed by injecting

OVOC standards (*e.g.* IEPOX, HMHP, *etc.*) into the chamber. Both particle and vapor wall loss characterizations were performed at several RH conditions (4–85% RH). These characterizations have been described in more detail previously (Loza *et al.*, 2010; Nguyen *et al.*, 2014a).

Organic compounds were injected into the chamber by two methods. (1) For volatile compounds, a measured volume was injected with a micro-syringe through a septum into a clean glass bulb, and the evaporated standard was quantitatively transferred into the chamber by dry purified air. Gas introduction of VOCs (done for isoprene and methacrolein) by filling an evacuated bulb with the chemical vapor, backfilling with nitrogen gas, and characterizing with Fourier transform infrared spectrometry before injecting did not produce significantly different results than volume injection. (2) For semivolatile compounds, the solid or liquid standard was placed inside a two-neck flask, which was heated by a water bath (35–65 °C), and the headspace was carried into the chamber by dry purified air. The ToFCIMS or TripCIMS instruments measured the gas-phase mixing ratio of the semi-volatiles in real time as the compounds entered the chamber, and injection was halted when a satisfactory quantity was introduced. OVOCs were calibrated by the ToFCIMS and TripCIMS by methods described earlier (Paulot *et al.*, 2009a). The desired RH inside the chamber was achieved by flowing dry purified air through a water-permeable (Nafion) membrane humidifier (FC200, Permapure LLC), kept moist by recirculating 27 °C ultra-purified (18 M $\Omega$ , 3 ppb TOC) water (Milli-Q, Millipore Corp). Particles were atomized into the chamber as described for particle wall loss experiments. When hydrated particles were needed for experiments, particles were injected *via* an in-line, heated, wet-wall denuder into a chamber that has RH above the efflorescence point of the particular salt (Martin, 2000).

### **A.2.2 Instrumentation and Sampling Modifications**

Instruments were connected *via* sampling lines to both chambers through port holes in the enclosure as shown in Figure A.2. Sampling lines were capped when not in use. Inlet and tubing material were instrument specific, and included stainless steel (GTHOS and ToF-AMS), heated stainless steel and quartz (TDLIF), electro-polished steel and FEP Teflon (NO<sub>3</sub>CIMS), polyetheretherketone (PEEK) and Teflon (SRIToFMS), and perfluoroalkoxy polymer (PFA) Teflon (other instruments).

The duration of each experiment (*i.e.*, the level of oxidation that can be probed) was critically dependent on the net sampling flow rates at which air was withdrawn

from the chamber. Sampling strategies were developed to minimize the effective sampling flow rate from each instrument, in such a way that instrument responses were not significantly different than during field campaigns. In many cases, a common high-flow Teflon sampling line was used to minimize the residence time of gases through tubing, and smaller flows were sampled orthogonally by each instrument. In some cases, a duty cycle was used as needed.

Several modifications from field designs were utilized for chamber sampling. The modifications were that (1) the GTHOS detection system was located between the chambers inside of the enclosure to minimize the residence time of  $\text{HO}_x$  inside the instrument (Figure A.2). The detection system was connected to the laser on the outside of the enclosure *via* a 3 m fiber optic cable fed through the side port hole. The sampling flow rate was similar to field flows (6 SLM); however, the fast-flow inlet was situated horizontally ( $\sim 2$  m in height) instead of vertically. The inlet was adapted to each bag directly, by attaching it to a Teflon plate that was in turn secured to the chamber walls *via* a large o-ring. The GTHOS inlet switched from Chamber 1 to Chamber 2 as needed. Chemical zeroing was performed by releasing hexafluoropropene ( $\text{C}_3\text{F}_6$ ) into the inlet as an OH scrubber, and dark zeroing by measuring the difference between online and offline signals. Chemical and dark zeroing methods were used to distinguish between OH present in the chamber or atmosphere (chemical OH) and OH that may have been produced after the gas stream enters the instrument, which is additional to the chemical OH signal; (2) LIF-OHR was diluted a factor of 10 with nitrogen gas (effective flow 6 SLM); (3)  $\text{NO}_3\text{CIMS}$  was diluted a factor of 5 with scrubbed zero air (effective flow 2 SLM); (4) GlyLIP and FormLIF both operated at 5 SLM instead of the usual 17 and 10 SLM, respectively; and (5) SRIToFMS (1.5 SLM) and GCFID (0.1 SLM) occasionally sampled through a 0.125–0.2500 OD PFA Teflon tube that was submerged in a cold bath kept at  $-40$  °C in order to remove interferences from certain OVOC (see Section A.2.3).

GC-ToFCIMS, first described in Bates *et al.* (2014), is an extension of the ToFCIMS. Analyte gas samples were focused with a cold trap onto the head of a RTX 1701 column (Restek) and eluted with a temperature ramping program (30–130 °C) in the oven before reaching the ToFCIMS for mass spectrometry detection. GC-ToFCIMS recorded data only when isomer separation was needed, because its operation took the standard scanning mode of the ToFCIMS offline. All other instruments operated normally with the following sampling flows: TDLIF

(4 SLM), ToFCIMS and TripCIMS (2 SLM), CRM-OHR (0.5 SLM), NO-CL (1 SLM), and IACIMS (2 SLM). Frequencies of zeroing (with dry N<sub>2</sub> or ultrazero air) and calibration (various methods) were instrument specific, with some instruments zeroing once per hour and calibrating once every few hours and others performing zeroing/calibration between experiments.

### A.2.3 Experimental Design

The experiments performed at FIXCIT can be divided into several categories, each probing one or more specific science questions outlined in Section A.1.2. Every experiment included successful elements from past studies, but with a special focus on extending to atmospheric conditions. One example is reducing the occurrence of RO<sub>2</sub> + RO<sub>2</sub> side reactions in chamber experiments, which can lead to yields of atmospherically relevant products that are biased low. Enabled by the high sensitivity of field instruments, photooxidation was performed with precursor mixing ratios as low as 12 ppbv. Certain instruments that required extensive dilution in a chamber setting, *e.g.* LIF-OHR, had poorer-quality data for low loading experiments. Experimental durations were typically 4–6 h, with the exception of overnight runs where the majority of instruments sampled briefly to establish starting conditions, then were taken offline during the nighttime and resumed sampling in the morning. The typical reaction time for an overnight experiment was ~15 h. Experimental details are reported in Table A.2. OH concentrations were derived from hydrocarbon decay data from GCFID, SRI-ToFMS, or ToFCIMS, when available, using published rate coefficients (Atkinson *et al.*, 2006; Bates *et al.*, 2014; Lee *et al.*, 2014). Otherwise, preliminary GTHOS chemical-zeroing data were used. The following types of experiments were included in the study:

**A. Blank (Expts. 4b and 5b):** blank experiments were designed to investigate background signals present in experiments that may have sources other than gas-phase chemistry of the injected hydrocarbon, *e.g.* from heterogeneous oxidation of residual organics on the chamber walls. OH precursors, such as hydrogen peroxide, were added to each chamber, the UV lamps were turned on, and sampling occurred as usual. Furthermore, the temperatures inside the chambers were ramped from 25 to 35 °C to explore the extent to which elevated temperatures change the chamber background signals due to increased volatilization of organics. Blank experiments were performed under dry conditions. Common background compounds produced from heterogeneous wall reactions are formic acid and acetic acid.

expt. #	expt. type	HC precursor	[HC] <sub>i</sub> (ppb)	Ox source	[OH] <sub>ss</sub> (# cm <sup>-3</sup> )	[O <sub>3</sub> ] <sub>i</sub> (ppb)	[NO] <sub>i</sub> (ppb)	[NO <sub>2</sub> ] <sub>i</sub> (ppb)	[NO]/[HO <sub>2</sub> ]	Add'l inj.	Rxn T (°C)	RH (%)
2	b	ISOP	45	OH HP + hv	1.5 × 10 <sup>6</sup>	<5	<0.04	<2	1/7	-	27	<5
3	c	ISOP	100	OH HP + hv	2.4 × 10 <sup>6</sup>	<5	500	15	>100	-	26	<5
4a	i	ISOPOOHs	250	-	-	-	-	-	-	-	24	<3
4b	a	Blank C1	0	OH HP + hv	2.0 × 10 <sup>6</sup>	<5	<0.04	<3	1/6	-	27-33	<5
5a	i	ISOPNs	<13	-	-	-	-	-	-	-	24	<3
5b	a	Blank C2	0	OH HP + hv	2.0 × 10 <sup>6</sup>	<5	<0.04	<2	1/5	-	27	<5
6	e	ISOP	91	O <sub>3</sub> rxn	[OH] <sub>i</sub> ~ 1 × 10 <sup>6</sup>	615	<0.04	<3	-	-	25	<5
7*	d	ISOP	30	OH MN + hv	4.1 × 10 <sup>4</sup> , 4.8 × 10 <sup>6</sup>	<5	0.08	45	2, 6	-	40, 40	<5
9	f	ISOP	18	NO <sub>3</sub> NO <sub>2</sub> /O <sub>3</sub>	3.8 × 10 <sup>8</sup>	55	0.10	100	2-3	HCHO	26	<5
10	b	α-PIN	30	OH HP + hv	2.0 × 10 <sup>6</sup>	<5	<0.04	<2	1/10	-	27	<5
11	c	α-PIN	30	OH HP + hv	2.5 × 10 <sup>6</sup>	<5	85	10	>100	-	26	<5
13	f	α-PIN	30	NO <sub>3</sub> NO <sub>2</sub> /O <sub>3</sub>	4 × 10 <sup>8</sup>	75	0.17	150	1.5-8	HCHO	25	<5
14	e	ISOP	100	O <sub>3</sub> rxn	[OH] ~ 0	605	<0.04	<3	-	CHX	25	<5
16*	d	α-PIN	30	OH MN + hv	6 × 10 <sup>4</sup> , 4 × 10 <sup>6</sup>	<5	0.08	<3	2-3, 10	-	40, 40	<5
17	b, i	4,3-ISOPOOH	60	OH HP + hv	1.2 × 10 <sup>6</sup>	<5	<0.04	<3	1/5	-	26	<5
18*	d	ISOP	28	OH MN + hv	1.0 × 10 <sup>5</sup> , 4.3 × 10 <sup>6</sup>	<5	0.08	<3	2-3, >100	-	25, 26	<5
19	b, h	ISOP	60	OH HP + hv	1.0 × 10 <sup>6</sup>	<5	<0.04	<4	1/5	wet AS	28	51
21	b	ISOP	22	OH HP + hv	2.0 × 10 <sup>6</sup>	<5	<0.04	<2	1/10	-	27	<5
22	c	ISOP	100	OH HP + hv	2.3 × 10 <sup>6</sup>	<5	430	15	>100	-	27	<5
23	e	ISOP	90	O <sub>3</sub> rxn	[OH] <sub>i</sub> ~ 1 × 10 <sup>6</sup>	600	<0.04	<3	-	-	25	50
24	c, h, i	4,3-ISOPN	12	OH HP + hv	3 × 10 <sup>6</sup>	7	115	55	>100	wet AS	26	52
25	b	MAC	43	OH HP + hv	3 × 10 <sup>6</sup>	<5	<0.03	<3	1/10	-	28	<5
26	g, h	MAC	45	OH MN + hv	2 × 10 <sup>7</sup>	<5	3.5	50	10-20	MAE, wet AS	26	<5, 40
27	d, i	trans-β-IEPOX	60	OH MN + hv	7.3 × 10 <sup>6</sup>	<5	0.25	<3	2-5	-	25	<5
29	e	ISOP	91	O <sub>3</sub> rxn	[OH] ~ 0	610	<0.04	<4	-	CHX	25	38
30	g, h, i	Pinonald.	15	OH MN + hv	3.5 × 10 <sup>6</sup>	<5	0.50	<3	4-8	-	26	<5

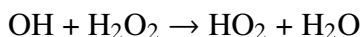
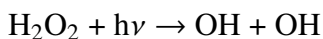
Table A.2: Formal experiments and reaction conditions during the FIXCIT campaign. Chemical abbreviations are defined in Table A.3. Other abbreviations are C1 = Chamber 1, C2 = Chamber 2, ISOP = isoprene, α-PIN = α-pinene, HP = hydrogen peroxide, MN = methyl nitrite, CHX = cyclohexane, HCHO = formaldehyde, AS = ammonium sulfate seeds. Expt. types are defined in the text. Expt. no. corresponds to the date in January 2014 when the experiment was performed. \* = 1% lights, 20% lights, then 100% lights.

synthesized standard	PI(s)	institutions	atmos. relevance	ref.
isoprene 1-hydroxy-2-hydroperoxide (1,2-ISOPOOH)	F. N. Keutsch	UWM	major 1st-gen. low-NO isoprene + OH product	a
isoprene 3-hydroxy-4-hydroperoxide (3,4-ISOPOOH)	F. N. Keutsch	UWM	major 1st-gen. low-NO isoprene + OH product	a
<i>trans</i> isoprene 2-epoxy-1,4-diol ( <i>trans</i> - $\beta$ -IEPOX)	P. O. Wennberg, J. H. Seinfeld	Caltech	major 2nd-gen. low-NO isoprene + OH product	b
<i>cis</i> isoprene 2-epoxy-1,4-diol ( <i>cis</i> - $\beta$ -IEPOX)	P. O. Wennberg, J. H. Seinfeld	Caltech	major 2nd-gen. low-NO isoprene + OH product	b
isoprene 4-hydroxy-3-nitrate (4,3-ISOPN)	R. C. Cohen, P. B. Shepson, A. S. Hasson, P. O. Wennberg	UCB, Purdue Univ., CSU Fresno (CSUF), and Caltech	major 1st-gen. high-NO isoprene + OH product	c
isoprene 2-hydroxy-1-nitrate (1,2-ISOPN)	A. S. Hasson	CSUF	major 1st-gen. high-NO isoprene + OH product	N/A
pinonaldehyde	P. O. Wennberg, J. H. Seinfeld	Caltech	major 1st-gen. $\alpha$ -pinene + OH/O <sub>3</sub> product	d
methacrylic acid epoxide (MAE)	J. D. Surratt, A. Gold	Univ. of NC Chapel Hill	minor product, possible SOA precursor from MAC + OH + NO <sub>2</sub>	e

Table A.3: List of contributed synthesized chemical standards for experiments and calibration. Synthesis references are <sup>(a)</sup>Rivera-Rios *et al.* (2014), <sup>(b)</sup>Bates *et al.* (2014), <sup>(c)</sup>Lee *et al.* (2014), <sup>(d)</sup>Griesbaum *et al.* (1997), and <sup>(e)</sup>Lin *et al.* (2013b).



**B. Low-NO photooxidation (Expts. 2, 10, 17, 19, and 25):** the low-NO experiments that have been extensively investigated in atmospheric chamber studies were designed to be relevant to the pristine troposphere, and certain conditions at SOAS, where HO<sub>2</sub> reactions dominate the RO<sub>2</sub> fate. Experiments were initiated by H<sub>2</sub>O<sub>2</sub> photolysis as a NO<sub>x</sub>-free source of OH and HO<sub>2</sub>:



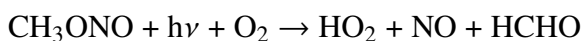
The execution of these experiments requires precise engineering to simulate the troposphere closely. One outstanding challenge of low-NO experiments is the variation in initial NO levels across different chamber settings and on different days. Because typical HO<sub>2</sub> levels in a chamber environment do not typically exceed ~200 pptv from the self-limiting HO<sub>2</sub> recombination, NO should be ~40 pptv during the reaction (a factor of 5 less abundant) in order for the C<sub>5</sub> RO<sub>2</sub> reactions to be dominated by HO<sub>2</sub> by a factor of 10 ( $k_{\text{RO}_2+\text{HO}_2} \sim 1.6 \times 10^{-11}$  and  $k_{\text{RO}_2+\text{NO}} \sim 8.5 \times 10^{-12} \text{ cm}^3 \text{ molec}^{-1} \text{ s}^{-1}$  at 298K (Atkinson *et al.*, 2006). Thus, experimental variations in NO that can lead to discrepancies in low-NO kinetics typically elude quantification by commercially available NO chemiluminescence instruments, owing to their high limits of detection (~500 pptv).

NO levels in the Caltech chambers were suppressed by continually flushing with filtered air on the inside and outside the chamber walls. Initial NO levels of <40 pptv were typically achieved during experiments. The NO-CL instrument available during FIXCIT (Table A.1) has a limit of detection better than 25 pptv, and the GTHOS instrument provided online HO<sub>2</sub> quantification at the pptv level. Another common challenge for low NO experiments (even when [NO] is less than [HO<sub>2</sub>]) is that homogeneous or cross RO<sub>2</sub> + RO<sub>2</sub> reactions may dominate the RO<sub>2</sub> reactivity ( $k_{\text{RO}_2+\text{RO}_2} \sim 10^{-15} - 10^{-11} \text{ cm}^3 \text{ molec}^{-1} \text{ s}^{-1}$  at 298 K; Atkinson *et al.*, 2006). These experiments may be more correctly characterized as "low-NO, high-RO<sub>2</sub>". For experiments using [H<sub>2</sub>O<sub>2</sub>] as an OH precursor, RO<sub>2</sub> + RO<sub>2</sub> reactions were largely minimized by using reaction conditions that ensure [HO<sub>2</sub>] greater than [RO<sub>2</sub>] (*e.g.*  $[\text{H}_2\text{O}_2]_0/[\text{ISOP}]_0 \sim 10^2$  and  $J_{\text{H}_2\text{O}_2} \sim 4-5 \times 10^{-6} \text{ s}^{-1}$ ). Thus, the peroxy radical self reaction channels are minor compared to RO<sub>2</sub> + HO<sub>2</sub> chemistry. We estimate that the low-NO experiments were HO<sub>2</sub>-dominated by at least a factor of 10 in RO<sub>2</sub> reactivity by monitoring tracers of chemistry stemming from high-NO (isoprene nitrates), high-RO<sub>2</sub> (C<sub>5</sub> diols and other products), and low-NO (ISOPOOH and IEPOX) pathways. The molar yield of the low-NO products ISOPOOH + IEPOX (measured

within the first 15 min of reaction) was estimated at 95%, supporting the dominance of  $\text{RO}_2 + \text{HO}_2$  chemistry over other channels. The structurally isomeric ISOPOOH and IEPOX that were formed from the  $\text{HO}_2$ -dominated isoprene photooxidation were distinguished by TripCIMS, and the sum was measured by ToFCIMS, IACIMS, and  $\text{NO}_3$ CIMS. These experiments were performed with isoprene,  $\alpha$ -pinene, 4,3-ISOPOOH and MAC precursors.

**C. High-NO photooxidation (Expts. 3, 11, 22, and 24):** high-NO experiments are also commonly performed in chamber studies. These experiments were designed to be relevant to the urban-influenced troposphere, such as some cases at SOAS, where NO can dominate  $\text{RO}_2$  reactions. Experiments were typically initiated by  $\text{H}_2\text{O}_2$  with added NO during FIXCIT, but have been performed using HONO or other precursors elsewhere. It is easier to ensure that reaction with NO is the main fate of  $\text{RO}_2$ , even with higher hydrocarbon loadings, because NO mixing ratios are typically in excess of both  $\text{HO}_2$  and  $\text{RO}_2$  by hundreds of ppbv. Hydroxy nitrate products were measured by TDLIF, IACIMS, ToFCIMS, and GC-ToFCIMS. Functionalized carbonyl products were measured by SRI-ToFMS and ToFCIMS. glyoxal and formaldehyde, also important high-NO products, were measured by the GlyLIP and FormLIF, respectively. This well-studied experiment was important for multiple reasons, including calibration, diagnostics, and for determining the hydroxy nitrate yields from alkenes within the first few minutes of photooxidation. However, it should be noted that the experimental result represents a boundary condition that may not fully represent NO-influenced reactions in the atmosphere due to the extremely short  $\text{RO}_2$  lifetimes ( $<0.01$  s at 500 ppbv NO). These experiments were performed with isoprene,  $\alpha$ -pinene, and the 4,3-ISOPN standard synthesized by the Caltech group.

**D. Slow chemistry photooxidation (Expts. 7, 16, 18, and 27):** the slow chemistry experiment is designed to extend  $\text{RO}_2$  lifetimes closer to atmospheric values when both NO and  $\text{HO}_2$  impact  $\text{RO}_2$  reactivity ( $\sim 3\text{--}30$  s, assuming 1500–100 pptv NO and 40 pptv  $\text{HO}_2$ ). This was achieved by employing low radical mixing ratios. With relevant  $\text{RO}_2$  lifetimes, the  $\text{RO}_2$  isomers may be closer to their equilibrium distribution because of the reversible addition of oxygen (Peeters *et al.*, 2009). Figure A.3 shows the progress of a representative slow chemistry experiment. The "slow" portion of experiments was performed under a low light flux ( $J_{\text{NO}_2} \sim 4 \times 10^{-5} \text{ s}^{-1}$ ) with methyl nitrite as the OH precursor (Atkinson *et al.*, 1981):



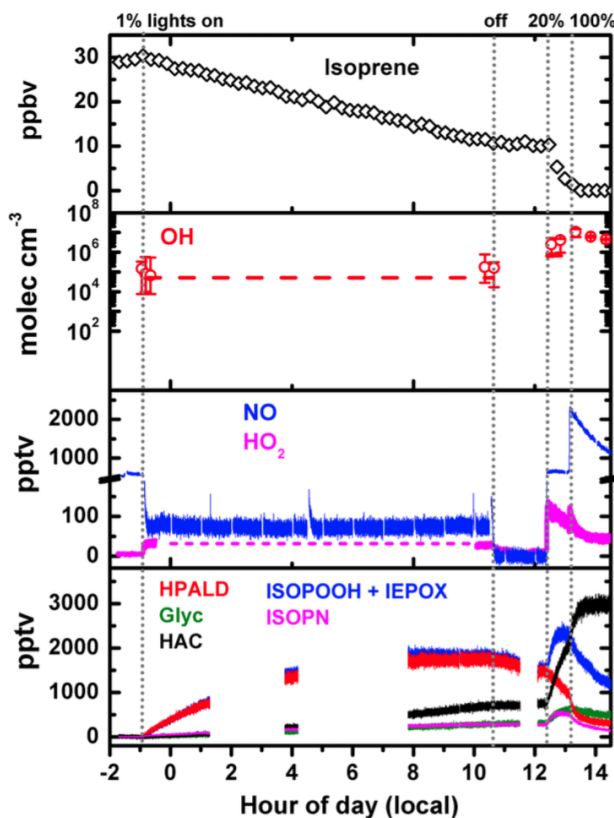
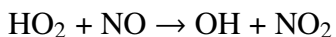


Figure A.3: Progress of the slow chemistry experiment performed on 01/07/2014. Isoprene data were provided by GCFID. The red dashed line in the OH plot is the steady-state OH concentration derived from the decay of isoprene as monitored by GCFID. OH and HO<sub>2</sub> preliminary data were provided by GTHOS, using chemical zeroing, although the steady-state value of  $(0.4\text{--}1) \times 10^5$  molec cm<sup>-3</sup> was below the detection limit of GTHOS. OH preliminary data were averaged to reduce noise. NO data were provided by NO-CL and OVOC data were provided by ToFCIMS.



These reactions produce a steady-state OH concentration of  $[\text{OH}]_{ss} \sim 0.4\text{--}1 \times 10^5$  molec cm<sup>-3</sup> and an atmospherically relevant ratio of NO / HO<sub>2</sub> (2–3) that is stable throughout the majority of the experiment. Furthermore, we aimed to simulate the summer conditions at SOAS, where RO<sub>2</sub> isomerization is competitive with RO<sub>2</sub> + HO<sub>2</sub> and RO<sub>2</sub> + NO chemistry. Thus, most experiments of this type were performed at elevated temperatures ( $T \sim 40\text{--}45$  °C) to facilitate the isoprene RO<sub>2</sub> isomerization to HPALDs (Crouse *et al.*, 2011), as measured by ToFCIMS. The atmospheric RO<sub>2</sub> fates were qualitatively deduced by observations of their respective products during SOAS (forthcoming papers) and during other campaigns (Beaver *et al.*, 2012; Paulot *et al.*, 2009b; Wolfe *et al.*, 2012).

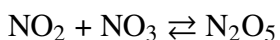
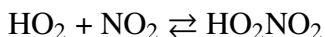
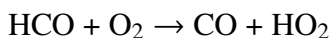
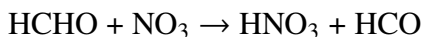
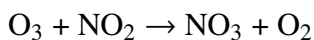
The fate of HPALDs is not known, but has been suggested as being strongly influenced by photolysis based on reactions of chemical analogs (Wolfe *et al.*, 2012). After the slow chemistry period, 20–100% lights were turned on in order to diagnose the effects of direct photolysis and OH oxidation on the product compounds, which is especially instructive when coupled with photochemical modeling. Table A.2 reports conditions only for the  $\leq 1\%$  light period and the 20% light period due to availability of hydrocarbon decay data. When CH<sub>3</sub>ONO experiments were performed with higher light flux from the start, the NO-to-HO<sub>2</sub> reactivities were still competitive, but the OH mixing ratios were higher. These experiments were performed with isoprene,  $\alpha$ -pinene, and *trans*- $\beta$ -IEPOX precursors.

**E. Ozonolysis (Expts. 6, 14, 23, and 29):** ozonolysis reactions were performed in the dark, with and without the use of excess cyclohexane (50 ppmv) as a scavenger for OH (Atkinson *et al.*, 1995). Ozone reacts with isoprene and  $\alpha$ -pinene with rate coefficients of  $k_{ISO+O_3} = 1.3 \times 10^{-17}$  molec cm<sup>-3</sup> and  $k_{\alpha-PIN+O_3} = 9.0 \times 10^{-17}$  molec cm<sup>-3</sup> at 298 K, respectively (Atkinson *et al.*, 2006). After the first few steps of the reaction, however, little agreement exists in the literature for product yields, product distribution, or rate coefficients stemming from reactions of stabilized Criegee intermediates (sCI). This may be due to the large differences among studies in the hydrocarbon loadings ( $[ISO]_i = 40\text{--}10\,000$  ppbv), ozone-to-isoprene ratios ( $<0.5$  to  $>100$ ), water vapor content ( $<10\text{--}20\,000$  ppmv), reaction pressures (4–760 torr), analytical methods used for product analysis (GC, HPLC, FTIR, direct OH vs. scavenging, *etc.*), and methods used to generate SCI (CH<sub>2</sub>I<sub>2</sub> + *h* $\nu$  vs. gas-phase ozonolysis) (Drozd and Donahue, 2011; Hasson *et al.*, 2001a; Huang *et al.*, 2013; Johnson and Marston, 2008; Kroll *et al.*, 2002; Neeb *et al.*, 1997; Sauer *et al.*, 1999; Simonaitis *et al.*, 1991; Welz *et al.*, 2012).

We designed the ozonolysis experiments to have similar ozone-to-isoprene ratios to those observed during SOAS ( $\sim 5\text{--}7$ ), and performed the experiments under dry (RH  $\sim 4\%$ ) and moderately humid (RH  $\sim 50\%$ ) conditions. The ozonolysis experiments at FIXCIT primarily focused on studying unimolecular and bimolecular chemistry of SCI that affects the yields of OH, hydroperoxides, organic acids, aldehydes and ketones under humid vs. dry conditions. These experiments represent the first coupling between direct OH observations from GTHOS, aldehyde/ketone measurements from GCFID and SRI-ToFMS, online formaldehyde measurements from FormLIF, and online hydroperoxide measurements from the various CIMS instruments present to provide the most comprehensive picture thus far on the

humidity-dependent ozonolysis of isoprene.

**F. Competitive HO<sub>2</sub> nitrate (NO<sub>3</sub>) oxidation (Expts. 9 and 13):** the NO<sub>3</sub>-initiated experiments during the campaign were performed in the dark, under dry conditions. Excess formaldehyde ([HCHO]<sub>i</sub> ~4–8 ppmv) was used as a dark HO<sub>2</sub> precursor in order to elevate the contributions of RO<sub>2</sub> + HO<sub>2</sub> reactions in the NO<sub>3</sub> chemistry:



This process produces an HO<sub>2</sub> / NO<sub>3</sub> ratio of approximately 2 (determined by photochemical modeling from the mechanism described in Paulot *et al.*, 2009a), a ratio more relevant to the troposphere during nighttime oxidation. As  $\alpha$ -pinene has a higher NO<sub>3</sub> loss rate compared to isoprene, a factor of 2 greater mixing ratio of initial formaldehyde was used. The consequence of the experimental design is that the isoprene nitrooxy hydroperoxide (INP) and monoterpene nitrooxy hydroperoxide (MTNP) are major products, in contrast to experiments performed under RO<sub>2</sub> + RO<sub>2</sub> or RO<sub>2</sub> + NO<sub>3</sub> dominated conditions (Kwan *et al.*, 2012; Ng *et al.*, 2008; Perring *et al.*, 2009). The focus of these experiments was the quantification of INP and MTNP with the various CIMS and with TDLIF, and further exploration of their loss channels to OH oxidation (simulating sunrise) or to dry AS seed particles by measuring organic aerosol growth on the ToF-AMS. These experiments were performed with isoprene and  $\alpha$ -pinene precursors.

**G. High NO<sub>2</sub>/NO photooxidation (Expts. 26 and 30):** the high NO<sub>2</sub>-to-NO ratios in the lower troposphere in most regions of the globe favor the production of acylperoxy nitrates (APNs) from the OH-initiated reaction of aldehydes like methacrolein and pinonaldehyde (Bertman and Roberts, 1991; Nozière and Barnes, 1998). Unlike the APN from methacrolein (MPAN), the APN from pinonaldehyde has never been measured in the atmosphere (Nouaime *et al.*, 1998; Roberts *et al.*, 1998; Wolfe *et al.*, 2012). The OH oxidations of aldehydes were performed with an NO<sub>2</sub> / NO ratio greater than 10, and NO<sub>2</sub> was replenished as it was reacted away. These reactions were initiated by CH<sub>3</sub>ONO photolysis under higher light flux, producing [OH] greater than 3 × 10<sup>6</sup> molec cm<sup>-3</sup>. Certain APNs were monitored with ToFCIMS, and total peroxy nitrates ( $\Sigma$ PNs) were monitored with TDLIF. A

major focus of the high NO<sub>2</sub> experiments was to investigate the SOA-formation potential and mechanisms from atmospherically relevant APNs, which is expanded in H.

**H. SOA-formation chemistry (Expts. 19, 24, 26, and 30):** experiments aimed specifically at studying chemistry leading to SOA formation have overlapping goals with those described above. One focus was the evaluation of the SOA-formation route from APNs by the proposed dioxo ketone, lactone, and epoxide mechanisms (Chan *et al.*, 2010a; Kjaergaard *et al.*, 2012; Lin *et al.*, 2013b), none of which has yet been validated by independent studies. However, the proposed epoxide chemistry has been integrated into some studies published soon after the proposal by Lin *et al.* (2013b) (Pye *et al.*, 2013; Worton *et al.*, 2013). After MPAN was formed from the high-NO<sub>2</sub> reaction of MAC + OH, a synthesized standard of methacrylic acid epoxide (MAE, provided by the UNC group), the proposed epoxide intermediate, was added to discern the SOA-forming potential of MAE vs. other reactive intermediates in the MPAN reaction. Following the injection and stabilization of MAE, water vapor was added until the reaction mixture reached ~40% RH. Then wet AS seeds were injected to investigate any SOA mass growth, as quantified by ToF-AMS.

SOA formation from ISOPN high-NO photooxidation and isoprene low-NO photooxidation products were investigated in the presence of wet AS seeds (40–50% particle liquid water by volume), meant to simulate the high particle liquid water and sulfate quantities during SOAS. For these experiments, the chambers were humidified to 40–50% RH, and hydrated AS particles were injected through a wet-wall denuder so that the seed particles retain liquid water above the efflorescence point of AS (Biskos *et al.*, 2006). In the ISOPN high-NO photooxidation, the potential for forming organics that will likely condense onto seed particles, *e.g.* dinitrates and IEPOX, was recently suggested (Jacobs *et al.*, 2014; Lee *et al.*, 2014). The dinitrate pathway was investigated as a potential source of particle-phase organic nitrogen. In the low-NO isoprene photooxidation, IEPOX reactive uptake onto acidic Mg<sub>2</sub>SO<sub>4</sub> particles (Lin *et al.*, 2012) and non-acidified AS particles (Nguyen *et al.*, 2014a), both with non-zero liquid water content, were recently demonstrated. We focused on AS particles with no added acid. The impact of the partitioning of IEPOX on the gas-phase mixing ratios was examined as a potential reason for the differences in observed IEPOX in dry and humid regions.

**I. Cross-calibrations (Expts. 4a, 5a, 24, 27, and 30):** newly commercially available negative-ion CIMS (Junninen *et al.*, 2010; Lee *et al.*, 1993b) may become

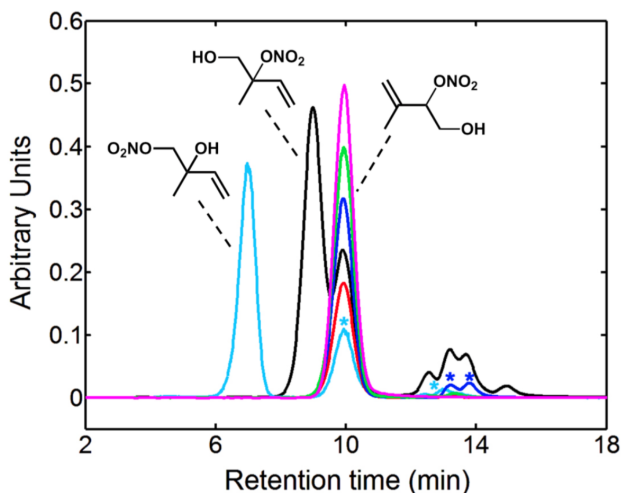


Figure A.4: GC-ToFCIMS chromatogram of ISOPNs from an isoprene high-NO photooxidation experiment (black), and from the introduction of 2,1-ISOPN standard synthesized by CSUF (cyan) and 4,3-ISOPN standards synthesized by Caltech (magenta), CSUF (green), UCB (blue), and Purdue (red). The rightmost four peaks apparent in the photooxidation chromatogram are preliminarily identified as the *cis* and *trans* 1,4-ISOPN and *cis* and *trans*-4,1-ISOPN, although the elution order is not clear. Asterisks (\*) denote impurities in synthesized samples of corresponding color.

common tools for monitoring complex OVOCs in the atmosphere, similarly to the widespread adoption of positive ion CIMS (PTR-MS-based instruments). Some of the new negative ion CIMS instruments were deployed for the first time in field campaigns occurring in recent years. During FIXCIT, synthesized standards of eight isomer-specific compounds were available for cross calibrations with different CIMS in order to better understand the chemical sources of ambient signals during SOAS and in other field campaigns. Table A.3 shows the structures, abbreviations, and contributors of the synthesized chemicals. The TripCIMS and the GC-ToFCIMS separated structural isomers through collision-induced dissociation (CID) and through chromatography, respectively. Figure A.4 shows a GC-ToFCIMS separation of isomers of the ISOPN synthesized standards, as well as ISOPNs present in a complex photooxidation mixture. SRI-ToFMS and IACIMS tested the switchable reagent ion sources for preferential detection of one or more isomers of compounds with the same molecular formula.

For certain cross-calibration experiments, standards were injected into an inflatable pillow bag ( $\sim 0.2\text{--}0.3\text{ m}^3$ ) that was filled with dry  $\text{N}_2$  to a known volume. The purities of the standards were quantified by nuclear magnetic resonance (NMR) or

Fourier transform infrared spectrometry (FT-IR). The injected material was measured by vapor pressure, quantitative volume transfer, or by ToFCIMS and TripCIMS that were calibrated using techniques described elsewhere (Bates *et al.*, 2014; Garden *et al.*, 2009; Lee *et al.*, 2014; Paulot *et al.*, 2009a). Some experiments, such as the IEPOX photooxidation experiment, also served a dual purpose for cross-calibration. For example, *trans*- $\beta$ -IEPOX was injected into a clean chamber and instruments were allowed to sample for  $\sim 1$  h to cross-calibrate before an oxidant precursor was injected. Both LIF-OHR and CRM-OHR were able to measure the OH reactivity of these OVOC compounds individually, which aids in determining the known and unknown OH reactivity in ambient environments.

**J. GTHOS test experiments:** the OH interference in GTHOS, and possibly other gas-expansion LIF techniques, has been shown to bias OH measurements systematically high in some biogenically influenced areas unless chemical zeroing was performed (Mao *et al.*, 2012). The excess OH was demonstrated not to be produced by the GTHOS laser itself (308 nm), but rather, more likely, in the low-pressure flow zone within the nozzle of the instrument. During FIXCIT, several hypotheses proposed by Mao *et al.* (2012), and some original proposals based on field observations, were tested. The interference precursor candidates were: (i) ozonolysis intermediates – tested with ozonolysis experiments and with ozone injection into the GTHOS inlet; (ii) biogenic peroxides like ISOPOOH or HMHP – tested with synthesized standards; (iii) background chemistry such as  $\text{NO}_2 + \text{O}_3$  – tested by the nitrate-oxidation experiment and by sequential injection of  $\text{NO}_2$  and  $\text{O}_3$  separately; (iv) dry and humid  $\text{HO}_2 + \text{O}_3$  reaction – tested by formaldehyde photolysis with ozone injection during a separate experiment (01/02/2014, not shown in Table A.2); (v)  $\beta$ -hydroxy  $\text{RO}_2$  radicals formed from OH + alkene – tested with the photooxidation of 2-methyl-2-butanol and compared with 2,2-dimethylbutane (02/02/2014 and 31/01/2014, not shown in Table A.2); and (vi) heat-mediated decomposition of thermally unstable species – tested by temperature ramping to 35–40 °C inside the chamber. Often, single variables (like ozone or heat) were isolated by incremental additions toward the end of an experiment.

The experiments not described in Table A.2 (to test iv and v) were performed after the formal experiments; thus, not all investigators were present. Only GTHOS, ToFCIMS, TripCIMS, ToF-AMS, GCFID,  $\text{O}_3$  monitor and  $\text{NO}_x$  monitor were collecting data. The  $\text{HO}_2 + \text{O}_3$  test experiment (01/02/2014) was performed by injecting  $\sim 600$  ppbv of ozone, then  $\sim 50$  ppbv of cyclohexane as an OH tracer for CIMS (mon-



itored by the formation of cyclohexyl hydroperoxide). UV lights were turned on and then 4 ppmv of formaldehyde was injected, which photolyzed to produce 550 pptv of HO<sub>2</sub>. The HO<sub>2</sub> reaction with formaldehyde produced a small yield of HMHP (Niki *et al.*, 1980). Water vapor was injected to diagnose the effect of humidity. Experiments to test the effects of RO<sub>2</sub> structure utilized CH<sub>3</sub>ONO to oxidize ~50 ppbv of either 2-methyl-2-butanol and 2,2-dimethylbutane with OH. Ozone (~ 600 ppbv), water vapor (until RH ~30–40%), and NO<sub>2</sub> (400 ppbv) were added sequentially at toward the end of the photooxidation. Finally severally hundred ppb of NO was added to titrate away the ozone.

#### A.2.4 Analytical Challenges

Throughout the campaign, several sources of analytical interferences or systematic biases were discovered. Some challenges resulted from the integration of field instruments to a chamber setting, where high concentrations of certain chemicals were used to engineer extremely specific conditions. Thus, these issues do not affect ambient sampling. For example, (1) high NO<sub>2</sub> levels in some experiments affected the normal operation of TDLIF because the ΣANs and ΣPNs measurements were determined by subtraction of NO<sub>2</sub>. When NO<sub>2</sub> is much higher than ΣANs and ΣPNs, the measurement by difference contains large uncertainties; (2) high H<sub>2</sub>O<sub>2</sub> for low-NO conditions affected the operation of some CIMS instruments because the ppmv mixing ratios of H<sub>2</sub>O<sub>2</sub> depleted a non-negligible quantity of reagent ions. In order to correct for this, the CIMS instruments needed to calibrate as a function of H<sub>2</sub>O<sub>2</sub> in addition to traditional methods, or account for the true reagent ion signal (which was anti-correlated with H<sub>2</sub>O<sub>2</sub> concentration). High H<sub>2</sub>O<sub>2</sub> also affected GTHOS due to photolysis-derived OH production by the laser. GTHOS corrected for this effect by removing the OH background that was determined by sampling when only H<sub>2</sub>O<sub>2</sub> was present; (3) High formaldehyde, cyclohexane, or H<sub>2</sub>O<sub>2</sub> dominated the OH reactivity for certain experiments. In experiments where ppmv levels of volatile compounds were used, LIF-OHR and CRM-OHR did not operate. In contrast, high ozone and NO levels did not appear to affect the operation of any instruments. Temperature and humidity effects on ion sensitivities have been corrected for by ToFCIMS and TripCIMS as standard procedure. Other CIMS are actively characterizing these effects for analytes of interest.

However, other analytical challenges were not unique to laboratory studies. It was found that chemical artifacts were produced from the decomposition of multifunctional OVOC (*e.g.* ISOPN, ISOPOOH, IEPOX, and pinonaldehyde) under normal

operating conditions in some instruments; thus, possibly affecting ambient sampling and field data interpretation. Figure A.5 shows the proposed decomposition pathways of certain isomers of isoprene-derived OVOC to form MAC and MVK. We are aware of MAC and MVK interference only from the 1,2- and 4,3- isomers of ISOPOOH, the 1,2- and 4,3- isomers and ISOPN, and the  $\beta$  isomers of IEPOX (*i.e.*, the peroxide, nitrate, and epoxide groups are secondary or tertiary). Unfortunately, these isomers are expected to be the most abundant in the atmosphere, *e.g.* the  $\beta$ -IEPOXs are estimated to represent more than 97% of atmospheric IEPOX (Bates *et al.*, 2014). The extent of decomposition and product distribution may also vary based on the operating conditions of the particular analytical method. In general, the decomposition was exacerbated by instruments with harsher sampling conditions, *i.e.*, high ionization energy (*e.g.* the standard  $\text{H}_3\text{O}^+$  mode of SRI-ToFMS), high temperatures, and/or materials incompatible with organics (*e.g.* the hot stainless steel sample loop and inlet of GCFID). OVOCs from the low-NO isoprene photooxidation have been shown to decompose to MAC and MVK in commercial PTRMS instruments (Liu *et al.*, 2013), but the exact identities of the compounds were unclear. During FIXCIT, it was observed that ISOPOOH, IEPOX, and pinonaldehyde were detected at  $m/z$  71.050 in the SRI-ToFMS in PTR mode (the sum of MAC + MVK). Switchable reagent ions show promise for removing certain biases, but more work is needed to characterize the chemistry that forms interfering ions. Furthermore, we observed that the decomposition interference also affected GCFID, the other commonly used detection method for MAC and MVK in ambient samples. ISOPOOH, IEPOX, and ISOPN were detected as either MAC or MVK in the GCFID, depending on the specific isomer. The interferences may not be localized to this particular GCFID, and a more detailed account can be found in Rivera-Rios *et al.* (2014). Conversion efficiencies of OVOCs to the  $\text{C}_4$  carbonyls in the Caltech GCFID range in order of ISOPOOH > IEPOX > ISOPN, and can be almost quantitative for ISOPOOH because of the facile cleavage of the weak O–O bond. Lastly, ISOPN were found to be converted to NO with a small yield in the NO–CL and a larger yield in commercial  $\text{NO}_x$  analyzers.

All decomposition-derived artifacts can be avoided by collecting the air sample through a length of tubing submerged in a cold bath ( $-40\text{ }^\circ\text{C}$ ), which trapped OVOCs that are less volatile than authentic MAC and MVK. Liu *et al.* (2013) implemented this technique successfully in their laboratory study using SRI-ToFMS, resulting in a lower yield than previously reported for MAC and MVK in the low-NO oxidation of isoprene. Field application may prove more challenging, however, as the trapping

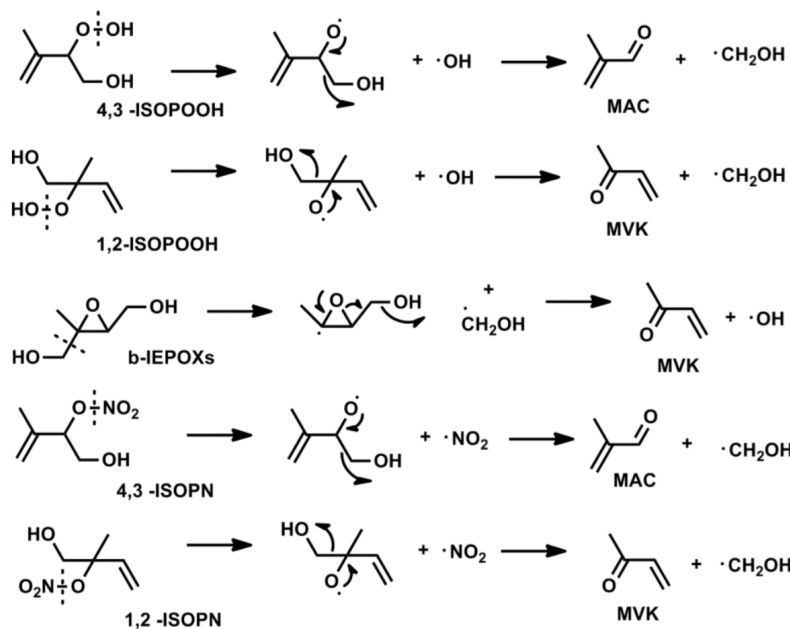


Figure A.5: Select proposed mechanism for the decomposition of OVOCs to carbonyls on contact with metal surfaces or high ionization energies within instrumentation. Other decomposition pathways likely exist and the branching ratios are dependent on instrument operation conditions. Cleavage sites are indicated by dashed lines.

is labor intensive and requires careful humidity control to avoid ice buildup and blockage. During FIXCIT, both GCFID and SRI-ToFMS employed trapping techniques at various times to avoid biases in the detection and interpretation of MAC and MVK data.

### A.3 Preliminary Results and Atmospheric Implications

Forthcoming papers will discuss campaign results in detail. Here, we summarize a few interesting observations that appeared to be robust, based on preliminary data analysis of the laboratory and field work.

– Nighttime chemistry of alkenes, as controlled by the  $\text{NO}_3$  radical, leads to several organic nitrates that are unique compared to daytime high-NO photooxidation. A significant product is the nitrooxy hydroperoxide, the atmospheric importance of which has likely been significantly underestimated in past chamber studies. The nitrooxy hydroperoxide reacts further in the daytime through a currently unknown mechanism.

– The high-NO hydroxy nitrate yield from isoprene is closer to the high end of the

spectrum (range 4–15%), important for the accurate simulations of volatile nitrogen in the atmosphere.

– Observed mixing ratios of isoprene low-NO photooxidation products are impacted by heterogeneous chemistry that appears to be mediated by aqueous processes, which has implications for the interpretation of IEPOX observations in dry vs. humid areas of the world.

– Environmental conditions in many locations, including within a biomass burning plume, are favorable for the H-shift RO<sub>2</sub> isomerization chemistry that produces compounds like HPALDs and very low-volatility oxygenates. The atmospheric fate of HPALDs is highly impacted by direct photolysis that recycles OH, as well as other complex chemistry and physical processes.

– The ozonolysis reaction of isoprene produces a high yield of C<sub>1</sub> compounds that are also observed with considerable abundance during ambient sampling. The hydroperoxide and acid yields appear to be underestimated by previous studies that detected these compounds *via* offline techniques. The OH yield may not follow the same trend with RH as the hydroperoxide and acid yields.

– APNs are efficient SOA precursors. SOA formation was prompt, and organic mass growth occurred quickly without the addition of inorganic seeds, *i.e.*, the SOA intermediate(s) from APN + OH condensed onto predominantly organic SOA material. Injections of the MAE standard did not increase the SOA mass growth.

– Several experiments produced significant amounts of excess OH, as measured by the GTHOS instrument, providing further avenues for investigation. These experiments also ruled out several candidates for the OH interference. More work is underway to characterize the phenomenon comprehensively.

– Calibrations with several synthesized standards of OVOC (Table A.3) significantly aid in data interpretation from OHR and new CIMS instruments. Sampling these OVOC through standard instrumentation may interfere with some routine field and chamber measurements (depends on the run conditions and instrument setup), but may be mediated by cold-trapping methods. This is likely a contributing factor in the high discrepancies in MAC and MVK yields from low-NO isoprene photooxidation previously reported. For example, we find the preliminary low-NO yields of MVK ( $6 \pm 3\%$ ) and MAC ( $4 \pm 2\%$ ), determined by GC-FID, from photooxidation of isoprene are consistent with Liu *et al.* (2013) when cold-trapping methods were employed (Expt. 21). However, the low-NO "yields" of MVK and MAC are each

greater than 40% when sampled directly by the GC-FID from the chamber (Expt. 2) due to interferences by isomers of ISOPOOH (Rivera-Rios *et al.*, 2014) and possibly other OVOCs.

Final data from the FIXCIT campaign will be made publicly available on archives hosted by the US National Oceanic and Atmospheric Administration (NOAA, <http://esrl.noaa.gov>) in January 2016. Data will be submitted in the ICARTT format, standardized by the US National Aeronautics and Space Administration (NASA, <http://www-air.larc.nasa.gov/missions/etc/IcarttDataFormat.htm>).

#### A.4 Summary

Although data analysis is ongoing, the goals of the FIXCIT campaign appear to have been met during the campaign period. The insights gained from experimental observations under well-controlled laboratory conditions have already proved valuable for understanding ambient observations from SOAS. The community effort to pursue atmospherically important chemistry with sensitive ambient techniques and custom-synthesized chemicals has elevated our understanding of atmospheric oxidation for a number of biogenic compounds. Novel mechanistic information obtained during FIXCIT will be helpful to update chemical mechanisms currently implemented in large-scale chemistry-coupled transport models. Instrumental inter-comparisons, an important aspect of the campaign, have demonstrated that a thorough characterization of new and standard ambient sampling techniques using authentic standards is necessary for accurate data interpretation.

Chamber experiments are clearly invaluable to the field of atmospheric chemistry, as the results feed directly into models that are used to ascertain regional and global climate and chemistry feedbacks. Furthermore, chamber data aid in the interpretation of complex results obtained from field studies. However, it can be difficult to decipher the conditions under which chamber experiments are most relevant, and a standard protocol for data reporting may be needed. For example, best estimates of oxidation conditions in chambers (*i.e.*, if reactions are HO<sub>2</sub>-dominated, low-NO but RO<sub>2</sub>-dominated, high-NO, high-NO<sub>x</sub> but low-NO, and so on) would greatly aid in comparisons of these experiments and others. The experiments in this campaign were fundamentally focused on the fate of the RO<sub>2</sub> radical as a delineation between chemical regimes. FIXCIT experiments (Table A.2) can be further improved or tailored to the specific needs of the scientist. It has been demonstrated, here and elsewhere, that chamber studies that include chemistry

representative of the atmosphere and well-characterized instrumental methods can accurately reproduce observations in the ambient environment. The results from FIXCIT make a case for future synergistic integration of laboratory studies with field campaigns, which maximizes the level of mechanistic understanding and data confidence obtained from the combination of both types of studies.